AIAA JOURNAL
Vol. 44, No. 10, October 2006

Temperature Measurements Using a Microoptical Sensor Based on Whispering Gallery Modes

G. Guan
World Precision Instruments Inc., Sarasota, Florida 34232
and
S. Arnold and M. V. Otugen
Polytechnic University, Brooklyn, New York 11201

DOI: 10.2514/1.20910

Temperature measurements were made using a novel microoptical sensor based on dielectric microspheres that are excited by coupling light from optical fibers. The technique exploits the morphology-dependent shifts in resonant frequencies that are commonly referred to as the whispering gallery modes. A change in the temperature of the microsphere leads to a change in both the size and the index of refraction of the sphere which results in a shift of the resonant frequency. By monitoring this shift, the temperature of the environment surrounding the sphere can be determined. The whispering gallery mode shifts are observed by scanning a tunable diode laser that is coupled into the optical fiber on one end and monitoring the transmission spectrum by a photodiode on the other. When the microsphere is in contact with a bare section of the fiber, the optical modes are observed as dips in the intensity of the light transmitted through the fiber. Temperature measurements were made in both air and water using this novel technique. Measurements by the microoptical sensor were compared to those by thermocouples with good agreement between the two sets of results

I. Introduction

OPTICAL microsphere resonators have attracted interest due to their unique properties including the very high quality factor they can exhibit. The quality factor, $Q = \lambda/\Delta\lambda$ (λ is the resonant wavelength), is a measure of how well an optical resonance [or whispering gallery mode (WGM)] of the sphere is resolved. Q values approaching a material loss limit of 10^{10} have been reported in the literature [1]. The very high values of Q allow for the determination of very small morphology dependent shifts in WGMs of optical spheres and raise the possibility of new sensor development. The morphological changes (such as size, shape, or the optical constants) of the sphere can be caused by a change in the physical condition of the surrounding. Therefore, by monitoring the WGM shifts, one may determine the change in a physical condition of the environment in which the microsphere is embedded. Several biological and mechanical sensing applications are possible using this optical phenomenon including temperature, pressure, and shear stress. One method to interrogate the WGMs is to couple laser light into the microsphere using optical fibers. Several applications of a WGM-based microsphere-fiber coupling system have been explored. These include laser frequency locking and stabilization [2], high-Q microphotonic electrooptic modulators [3], tunable optical filters for optical networks [4], and thermooptic switches based on WGM resonance tuning by temperature changes [5]. The concept of a WGM-based biosensor for protein detection has also been demonstrated [6–9]. In the mechanical sensing area, strain-induced tuning of WGMs was demonstrated by compressing a fiber-coupled sphere between piezoactivated pads [10] and most recently, a prototype force microsensor concept was demonstrated [11]. In this study, force resolution $\sim 10^{-2}$ N was obtained using solid silica microspheres.

A review of early literature on the behavior of morphology dependent shifts of WGM is provided by Hill and Benner [12]. Several theoretical analyses of the phenomenon have also been carried out in recent years [13–15].

In the present, we demonstrate a WGM-based temperature sensor. A schematic of the WGM-based sensor concept is shown in Fig. 1. The sensing element is the microsphere which is side coupled to an optical fiber as shown. The optical fiber, which carries light from a tunable laser, serves as an input/output port for the microsphere. When the microsphere comes into contact with an exposed section of the fiber core, its resonances are observed as sharp dips in the transmission spectrum as shown in Fig. 1. When the sphere is sufficiently close to the bare fiber, the evanescent fields of the sphere and the fiber overlap and light coupling occurs between the sphere and the fiber (in both directions). Thus, the microsphere-fiber system can be viewed as an interferometer similar to, for example, a Fabry–Perot instrument. The main difference is that it is much smaller, simpler to set up, and provides significantly larger Q values. Also, unlike the Fabry–Perot interferometer, the resonance condition is associated with dips in the transmission spectrum as opposed to peaks. The dips can be explained by the increased loss of electromagnetic energy in the sphere at the resonant condition. At resonance, the constructive buildup of the electromagnetic field in the sphere leads to increased losses (due to both material absorption and scattering) leading to the dips in the output light intensity. The dips (representing the WGMs), are extremely narrow due to the large Q factors and hence are highly sensitive to any change in the shape and size of the microsphere. A small change in the size and index of refraction due to a change in temperature of the microsphere will cause a shift in the WGM positions allowing for the precise measurement of temperature.

II. Measurement Principle

Light with vacuum wavelength λ is introduced into a dielectric microsphere of radius r and reflective index n, by side coupling it to a tapered optical fiber as shown in Fig. 1. Geometric optics representation of a WGM in a microsphere is shown in Fig. 2. Light circles the interior of the sphere through total internal reflection and returns in phase. For $r/\lambda \gg 1$, the condition for optical resonance (or WGM) can be approximated by $2\pi rn = \ell\lambda$ where ℓ, an integer, can be viewed as the ratio of the optical length completing one full trip to the wavelength. In terms of frequency, this condition is $\nu = (c/2\pi rn)\ell$ where c is the speed of light in vacuum. An incremental

Presented as Paper 7127 at the Infotech@AIAA, Arlington, Virginia, 26–29 September 2005; received 5 November 2005; revision received 5 June 2006; accepted for publication 6 June 2006.

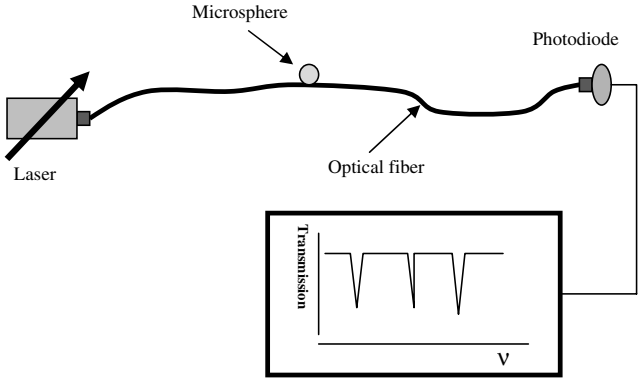

Fig. 1 Schematic of optical sensor and output signal.

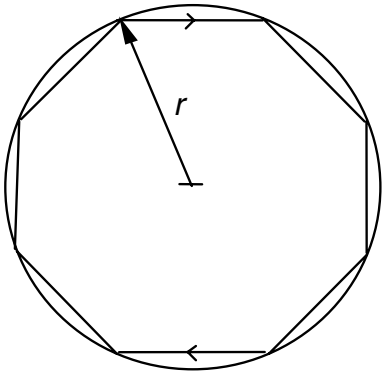

Fig. 2 Ray optics representation of WGM.

change in the index of refraction or radius of the sphere will result in a shift in the resonant frequency. Therefore, a change in any of the physical conditions of the surrounding area that induces a Δn or Δr on the microsphere can be sensed by monitoring WGM shifts. As discussed above, WGMs are observed as sharp dips in the transmission spectrum through the fiber (Fig. 1). The observed linewidth $\delta\nu$ of the WGM is related to the quality factor $Q = \nu/\delta\nu$. The smaller the energy loss as the light circulates inside the sphere, the larger Q is with $Q \to \infty$ as the losses vanish. One of the principle advantages of the WGM-based sensor concept is that WGMs of dielectric microspheres provide exceptionally large Q factors for the optical configurations shown in Fig. 1. Taking into account material losses, Q factors as high as 10^{10} are possible [1]. In practice Q factors in the range 10^7 and 10^8 have been reported [16]. Because the measured quantity is related to the shift in resonance, the observed linewidth essentially determines the measurement resolution.

A change in the temperature of the microsphere induces a change in both the radius of the sphere and in the index of refraction of the sphere material. Each of these will contribute to a shift in a resonance of the spheroid as follows:

$$\frac{\Delta\lambda}{\lambda} = \frac{\Delta(nr)}{nr} = \frac{\Delta r}{r} + \frac{\Delta n}{n} = \alpha\Delta T + \beta\Delta T = (\alpha+\beta)\Delta T \quad (1)$$

$$\Delta T = \frac{1}{\alpha+\beta}\frac{\Delta\lambda}{\lambda} \quad (2)$$

Here α is the thermal expansion coefficient while β is the thermal coefficient for index of refraction. For the present microspheres, $\alpha = 5.5 \times 10^{-7}{}^{\circ}\mathrm{C}^{-1}$ and $\beta = 8.53 \times 10^{-6}{}^{\circ}\mathrm{C}^{-1}$. Therefore, the change in the index of refraction is the dominant factor in the shift of the mode frequency. However, in calculating the temperature from the frequency shift, both effects should be taken into account.

If several physical parameters are changing simultaneously, they may all affect the WGM spectrum. For example, both temperature and pressure induce a change in the WGM as both induce a size change (but not a shape distortion). But, as pointed out previously, the temperature change also induces a strong perturbation in the index of refraction in addition to the radius change. Therefore, precisely how these resonances behave with a change in a given physical parameter is important in building sensors for specific applications. In the preliminary experiments presented in this paper, all other environmental conditions were kept constant while the temperature was varied.

For the range of practical interest covering microsphere radii of $5 \le r \le 200$ μm, with laser wavelength $\lambda \sim 1$ μm (corresponding to $30 \le l \le 1200$), we need to go beyond the geometric optics approximation and describe the resonances in terms of electromagnetic modes for a more comprehensive analysis. The solution to Maxwell's equation for a sphere provides three integer sets: n, ℓ, and m. Here n gives the number of nodes of the intensity distribution in the radial direction. ℓ, as described earlier, is approximately the number of wavelengths packed along the circumference of the sphere traveling along the equatorial belt of the sphere (parallel to the optical fiber). m is the azimuthal order number and can be viewed as the light traveling around the sphere surface on planes that make different azimuthal angles to the equatorial plane. For any value of ℓ, m varies as $|m| \le \ell$. For a perfect sphere with uniform index of refraction, all m modes have the same resonant wavelength as ℓ because planes at different azimuthal angles have the same circumference. Therefore, for a perfect sphere, the transmission spectrum will show only the ℓ modes that are separated by the free spectral range, $\mathrm{FSR} = c/(2\pi nr)$. Any deviation from the spherical shape or nonuniformity in the index of refraction will result in shifts of the m modes, hence, additional dips in the transmission spectrum.

III. Experimental Setup and Procedure

A. Experimental Setup

A schematic representation of the experimental setup is shown in Fig. 3. The setup consists of a scanning distributed feedback (DFB) laser, operating around 1306 nm wavelength (Mitsubishi ML725B11F), associated electronics to drive the laser, a single mode fiber, fiber couplers, the test section (which includes the spheroid microbead touching the fiber), a photodiode, A/D converter, and a personal computer. The laser frequency is scanned by changing the current applied to the laser diode. The laser driver provides a sawtooth input of current into the diode. The driver, in turn, is controlled by a function generator which provides a sawtooth voltage wave form for the driver. The laser output is coupled into the single mode fiber. The core diameter of the single mode fiber is ~ 8 μm. On the output side (past the test section), the light exiting fiber is coupled into a photodiode. The output of the photodiode is sampled using a 16-bit A/D converter and processed by the personal computer. The personal computer controls the measurement process including the scanning of the laser. The details of the test section are shown in Fig. 4. In the test section, a length of about 1 cm of the fiber is stripped of its cladding and the fiber is etched (using a 20–25% concentration of hydrofluoric acid) to a diameter, typically, of about

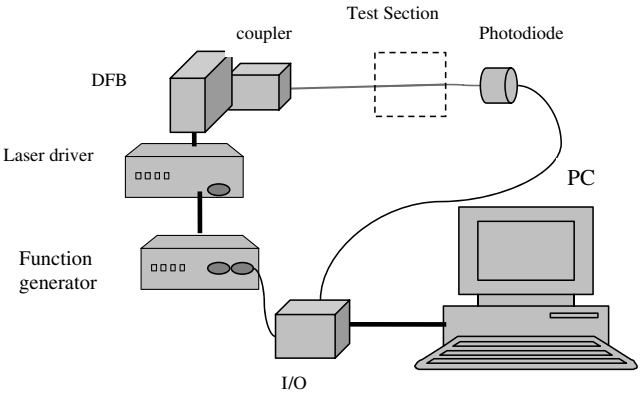

Fig. 3 Experimental setup.

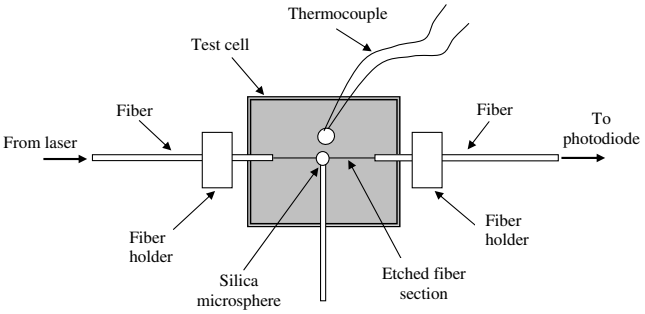

Fig. 4 Top view of test section.

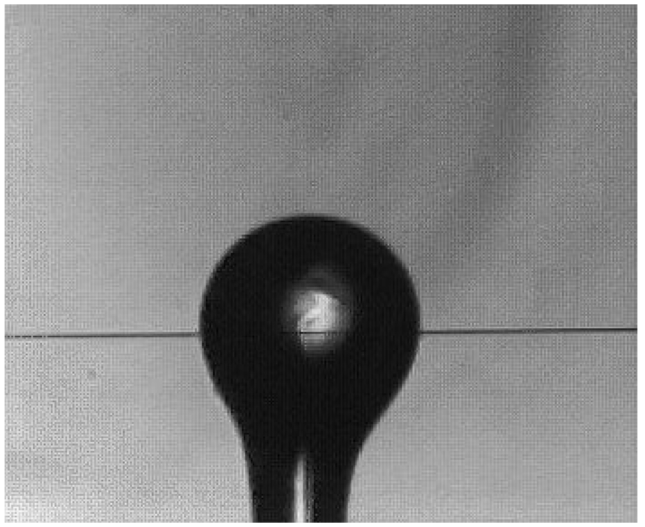

Fig. 5 Optical sensor.

4–5 μm. Separately, a silica bead with a stem is made by melting the tip of an optical fiber using a microflame torch. (The diameters of the beads used range between 150–400 μm.) The bead is placed near the middle of the etched portion of the fiber, just touching the fiber as shown in Fig. 5. In this figure, the fiber and bead diameters are $\sim$5 and $\sim$350 μm, respectively. This sensing system is placed in a test cell which can be either filled with water or just air. A thermocouple is also placed inside the cell adjacent to the silica bead to provide an additional independent measurement of the local temperature.

B. Resonance Detection and Tracking

The personal computer and an I/O board (consisting of the A/D and D/A converters) control the experiments. The ramp generator generates the scanning signal to the DFB laser. The output of the photodiode is digitized by the 16-bit A/D converter. A software program identifies and tracks each resonance in terms of its scanned laser wavelength. The shift in wavelength in each resonance is related to the temperature of the microsphere. The task is to identify

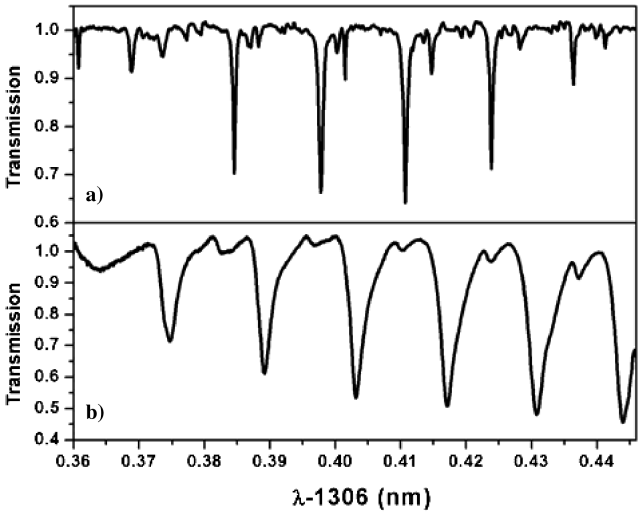

Fig. 7 Comparison of transmission spectra in air a) and in water b).

several of the dips (corresponding to the spherical modes) in the spectrum with the software and track their movement (change of the frequency of a given mode). Note that for the temperature range measured, the shift in modes is larger than the scanning range of the laser. Therefore the software has to first identify a number of the modes initially and then track each of the identified modes through temperature change. As modes leave the scanning range of the laser, and new modes come in the range, the software identifies them and their initial location and tracks their movement through the scanning range.

IV. Results

A typical transmission spectrum through the fiber with the microbead touching it is shown in Fig. 6. In this case, the "sensor" is in air. The laser is calibrated using a wave meter (input current to the laser versus actual wavelength of laser output). Note that the laser output power is a function of the wavelength; hence the nonnormalized spectrum on the left shows a pedestal. The spectrum on the right is that with the pedestal removed.

Figure 7 compares the transmission spectrum with the sensor in air a) to that in deionized water b). The resonance positions within a spectrum are determined by the characteristics of the microsphere WGMs. The linewidth is determined to be $\sim$1.2 pm [full width at half-maximum (FWHM)] for air in Fig. 7a, resulting in a Q value of the optical microcavity of about 1×10^6. The corresponding linewidth in Fig. 7b is larger ($\sim$2.2 pm FWHM) yielding a lower Q value of $\sim 6 \times 10^5$. The linewidth of the resonant dips (i.e., the Q factor) is dictated by several factors including the coupling condition [17]. But the main reason for the smaller Q value in Fig. 7b is the increased scattering losses in water. As the light travels inside the sphere through total internal reflection, there is a small amount of scattering loss at each reflection. This loss is a function of sphere-to-surrounding index of refraction ratio. Smaller ratios will lead to

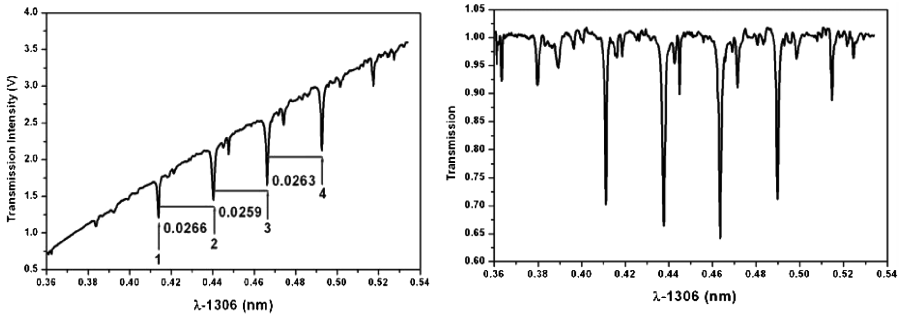

Fig. 6 Typical transmission spectrum in air.

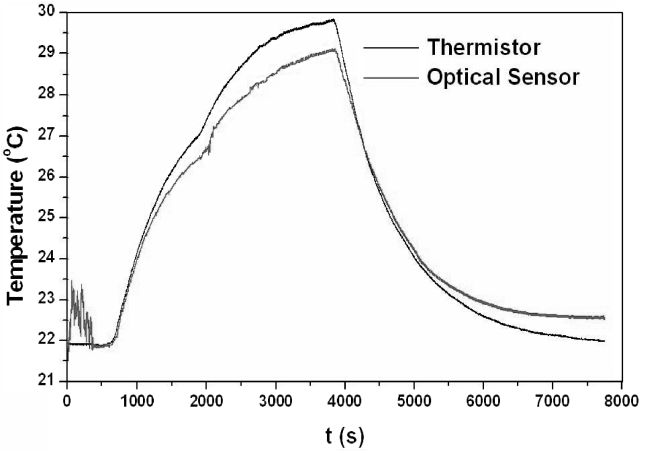

Fig. 8 Temperature measurement in water.

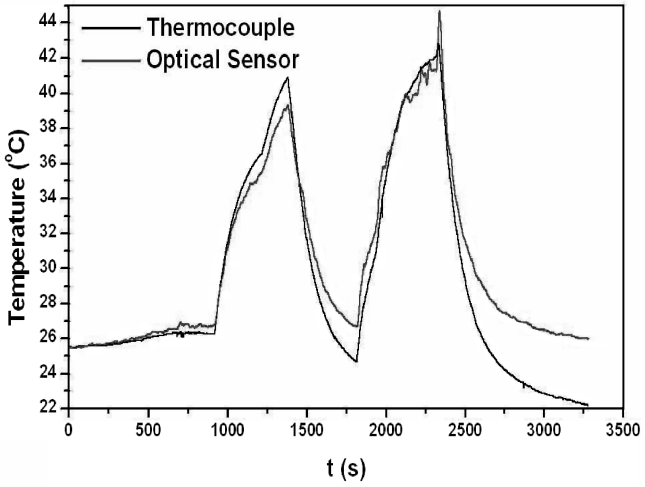

Fig. 9 Temperature in air.

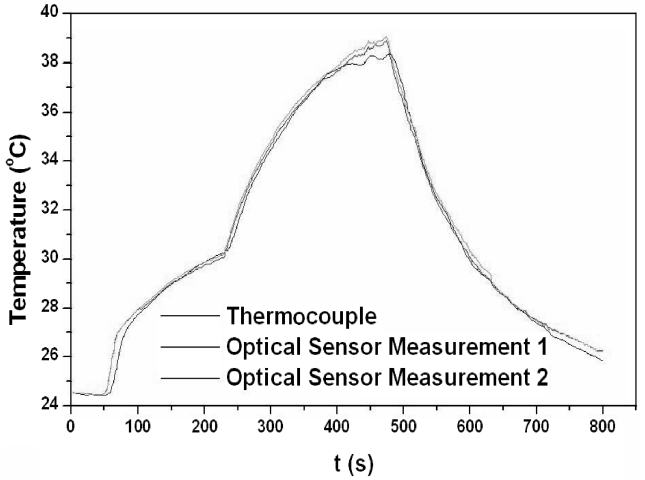

Fig. 10 Temperature measurement in air by two optical sensors simultaneously.

larger scattering losses. The index of refraction ratio is ∼1.47 for silica in air and ∼1.1 for silica in water

A. Temperature Measurements in Water

As a first step, we carried out temperature measurements in water. Because the thermal inertia of the water is significantly larger than that of air, the temperature changes are slower, hence it is easier to track temperature with the measurement system. In the water experiments, the test cell is filled with water. A thermistor is placed near the sphere to monitor the temperature of water as shown in Fig. 4. The bead, the fiber, and the thermistor are all immersed in the water. The function generator generates a ramp signal at 15 Hz repetition rate. The photodiode signal is sampled at 500 points for each ramp cycle. Sampling starts whenever an external trigger signal is received. A typical result is shown in Fig. 8. The experiment starts with the cavity at room temperature. Over a period of about an hour, the test section that includes the water with optical sensors inside it is heated using a heating tape that is placed on top of the test section. (The heating is applied from the top to minimize convection currents.) At the end of the hour, the heater is shut off and the test cell is allowed to cool down. The temperature for the optical sensor is determined using Eq. (2). For the initial value, the temperature from the thermocouple is used. The agreement between the optical sensor and the thermistor is good. The same temperature trends are captured by the optical sensor and the thermistor and the maximum disagreement between the two measurements is under 1°C. The small disagreement between the two measurements occurring near the peak temperature and at the end of the cooling period may be attributed to a possible shift in the position of the bead relative to the bare fiber. Even a slight shift in the relative bead-fiber position would result in a change in the launch angle of the light into the bead from the fiber, hence resulting in a shift of the resonant modes in the transmission spectra. Because the present experiments serve as proof of principle, no special attempt was made to fix the fiber position relative to the microsphere. Future research will investigate several encapsulation approaches to fix the fiber to the sphere.

B. Temperature Measurements in Air

Next we carried out measurements in air. In this case, the test cell just has air together with the optical sensor and a thermocouple. The thermocouple bead is ∼1 mm in diameter and hence has a thermal response time that is well under a second. A sample measurement is shown in Fig. 9. As in the case of Fig. 8, several resonances are followed at any given time (typically 3 or 4) and the mode shift is determined using the average of shifts of all the modes that are present within the scan range of the laser. In Fig. 9 the measurement starts at room temperature and then the heater is turned on. As shown, two cycles of heating and cooling are tracked. With the exception of the cooling period of the second cycle, the agreement between the thermocouple and the optical sensor is good. It is noted that near the end of each cooling period (particularly at the end of the second cycle), the agreement between the sensor and the thermocouple weakens. As in the case with water measurements, it is possible that during the cooling period the position of the bead relative to the bare fiber may have slightly shifted resulting in a shift of the resonant modes in the transmission spectra.

Figure 10 shows temperature measurement in air this time with two optical sensors placed in the same cell. Note that a single fiber is used. The two beads are placed side by side on the same etched fiber. The software is modified so that within the laser scanning range, it not only tracks a single mode (represented by a dip in the transmission spectrum) from each sensor but also recognizes which mode is from which bead and determines temperature from each sensor separately. The agreement among the two optical sensors and the thermocouple is quite good.

Next we measured two different temperatures by two beads (sensors) placed on the same optical fiber and the results are shown in Fig. 11. The fiber is etched at two locations approximately 7 cm apart (the etched portion at each location is again ∼1 cm). Each bead (sensor) is placed in a separate cell with a thermocouple adjacent to it.

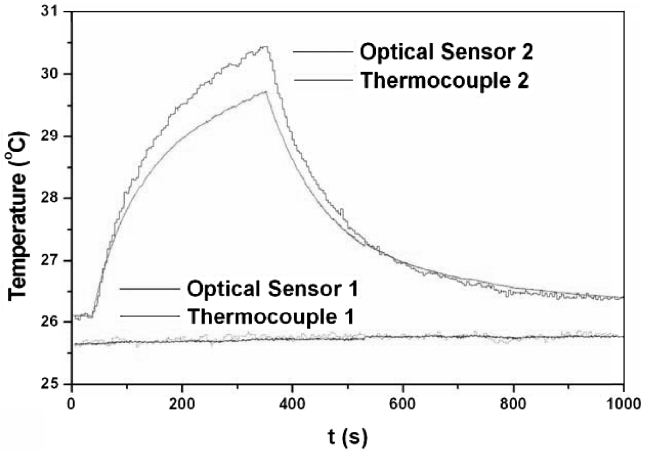

Fig. 11 Simultaneous measurement of temperature at two locations.

The same software as for Fig. 10 is used to track the temperature of each cell. One cell is heated while the other is kept at room temperature. It is clear that by using a single fiber with two beads it is possible to measure temperature at two locations. However, it would be difficult to measure temperature simultaneously at a large number of locations with this "series" (single fiber) approach because the present software would not be able to detect the movement of a large number of modes from the sensors. A more robust approach would be to use a "parallel" scheme. In this, the optical fiber from the laser is coupled into a number of parallel fibers each with a single sphere attached, using a fast scanning optical switch. The output of the parallel fibers is then combined into a single fiber, connected to the photodiode. We are currently investigating this scheme, which still uses a single laser and a detector.

V. Conclusions

A novel microoptical temperature sensor concept has been demonstrated. The technique is based on the detection of the so-called whispering gallery optical modes of dielectric microspheres that are coupled to optical fibers. The dielectric beads, which serve as the microspheres, typically have diameters of the order of several hundred micrometers and are of the same material as the optical fiber. The preliminary measurements indicate the viability of this approach for temperature sensing. The present study focuses on the measurement of temperature; however, sensors for other physical parameters such as pressure, force, and species concentration exploiting the same optical principle are possible.

Acknowledgement

This work was supported by the NASA Glenn Research Center (NASA Award NAG3-2679) with R. G. Seasholtz and G. Adamovsky as technical monitors.

References

[1] Geodesy, M. L., Sachiko, A. A., and Lichen, V. S., "Ultimate Q of Optical Microsphere Resonators," *Optics Letters*, Vol. 21, No. 7, 1996, pp. 453–455.

[2] Griffel, G., Arnold, S., Taskent, D., Serpenguzel, A., Connolly, J., and Morris, N., "Morphology-Dependent Resonances of a Microsphere-Optical Fiber System," *Optics Letters*, Vol. 21, No. 10, 1996, pp. 695–697.

[3] Cohen, D. A., Hossein-Zadeh, M., and Levi, A. F. J., "High-Q Microphotonic Electro-Optic Modulator," *Solid-State Electronics*, Vol. 45, No. 9, 2001, pp. 1577–1589.

[4] Savchenkov, A. A., Ilchenko, V. S., Matsko, A. B., and Maleki, L., "Tunable Filter Based on Whispering Gallery Modes," *Electronics Letters*, Vol. 39, No. 4, 2003, pp. 389–391.

[5] Tapalian, H. C., Laine, J. P., and Lane, P. A., "Thermooptical Switches Using Coated Microsphere Resonators," *IEEE Photonics Technology Letters*, Vol. 14, No. 8, 2002, pp. 1118–1120.

[6] Vollmer, F., Arnold, S., and Libchaber, A., "Novel, Fiber-Optic Biosensor Based on Morphology Dependent Resonances in Dielectric Micro-Spheres," *Biophysical Journal*, Vol. 82, No. 1, 2002, pp. 161A–162A.

[7] Vollmer, F., Braun, D., Libchaber, A., Khoshsima, M., Teraoka, I., and Arnold, S., "Protein Detection by Optical Shift of a Resonant Microcavity," *Applied Physics Letters*, Vol. 80, No. 21, 2002, pp. 4057–4059.

[8] Arnold, S., Khoshsima, M., Teraoka, I., Holler, S., and Vollmer, F., "Shift of Whispering-Gallery Modes in Microspheres by Protein Adsorption," *Optics Letters*, Vol. 28, No. 4, 2003, pp. 272–274.

[9] Teraoka, I., Arnold, S., and Vollmer, F., "Perturbation Approach to Resonance Shifts of Whispering-Gallery Modes in a Dielectric Microsphere as a Probe of a Surrounding Medium," *Journal of the Optical Society of America B (Optical Physics)*, Vol. 20, No. 9, 2003, pp. 1937–1946.

[10] Ilchenko, V. S., Volikov, P. S., Velichansky, V. L., Treussart, F., Lefevre-Sequin, V., Raimond, J-M., and Haroche, S., "Strain-Tunable High-Q Optical Microsphere Resonator," *Optics Communications*, Vol. 145, No. 1, 1998, pp. 86–90.

[11] Kozhevnikov, M., Ioppolo, T., Stepaniuk, V., Sheverev, V., and Otugen, V., "Optical Force Sensor Based on Whispering Galley Mode Resonators," AIAA Paper 2006-649, Jan. 2006.

[12] Hill, S. C., and Benner, R. E., "Morphology-Dependent Resonances," *Optical Effects Associated with Small Particles*, edited by P. W. Barber and R. K. Chang, World Sientific, Singapore, 1988.

[13] Lai, H. M., Leung, P. T., Young, K., Barber, P. W., and Hill, S. C., "Time-Independent perturbations for Leaking Electromagnetic Modes in Open Systems with Application to Resonances in Microdroplets," *Physical Review A*, Vol. 41, No. 9, 1990, pp. 5187–5198.

[14] Johnson, B. R., "Theory of Morphology-Dependent Resonances: Shape Resonances and Width Formulas," *Journal of Optical Society of America A*, Vol. 10, No. 2, 1993, pp. 343–352.

[15] Lam, C. C., Leung, P. T., and Young, K., "Explicit Asymptotic Formulas for the Positions, Widths, and Strengths of Resonances in Mie Scattering," *Journal of the Optical Society of America B (Optical Physics)*, Vol. 9, No. 9, 1992, pp. 1585–1592.

[16] Götzinger, S., Demmerer, S., Benson, O., and Sandoghdar, V., "Mapping and Manipulating Whispering Gallery Modes of a Microsphere Resonator with a Near-Field Probe," *Journal of Microscopy–Oxford, 2001*, Vol. 202, No. 1, 2001, pp. 117–121.

[17] Little, B. E., Laine, J. P., and Haus, H. A., "Analytical Theory of Coupling from Tapered Fibers and Half-Blocks into Microsphere Resonators," *Journal of Lightwave Technology*, Vol. 17, No. 4, 1999, pp. 704–715.

R. Lucht
Associate Editor